Building Tomorrow's Society
Bâtir la Société de Demain

Fredericton, Canada
June 13 – June 16, 2018/ *Juin 13 – Juin 16, 2018*

IMPROVING CONVEYANCE SIDE SLIPPER PLATE DESIGN TO ACCOMMODATE HIGHER IMPACT BUNTON FORCE

Hanna, Maykel[1,4], Lloyd, Alan[2] and Tikka, Timo[3]
[1] University of New Brunswick, Canada
[2] University of New Brunswick, Canada
[3] Stantec Ltd., Canada
[4] m.salib@unb.ca

Abstract: The demand on mine conveyances is increasing as material is being transported to the surface in larger quantities than ever. Mines are utilizing higher mass conveyances moving with higher hoisting speeds. Both contribute to potentially higher lateral impact forces from the conveyance onto the fixed guide system at the slipper location. The magnitude of these impact forces or slam loads needs to be minimized to mitigate potential damage to the guide rail system and allow continuous operation of mines. This research examined the behavior of Cotton Duck Pads (CDP), a type of elastomeric bearing pads, under impact load to be used to reduce the slam loads exercised on mine guide system. Fifty-two (52) specimens were tested to study the CDP behavior under strain rates of 0.001 to 200s $^{-1}$. The tests were conducted using a Universal Compression Testing Machine for low strain rates and a modified Charpy machine for high strain rates. This research, also, examined the dynamic behavior of conveyances using the Comro design guideline (1990) and compared it against single degree of freedom analysis using Newmark's method. The data, collected during different tests, were used to present stress-strain curves of CDP to be used in the dynamic analysis. To simplify the conveyance's dynamic analysis, secant value of modulus of elasticity (300-400 MPa) could be added to design practice. This article presents a design guideline for designing bearing pads used to reduce rare and extreme impact loads in a mineshaft.

1 INTRODUCTION

Mining structures are some of the most complex structures in the building field. Mineshafts are among the most important components of the infrastructure in a deep mine as they are used for transporting people and equipment to and from the mine core as well as lifting the raw materials to the surface. A steel system (steelwork) is used to divide the mineshaft area and provide guidance to the movement of conveyances between the surface and the mine core. This steelwork is comprising of horizontal bunton sets and vertical guides. The horizontal buntons are used to support the guides and transfer the loads of the hoisting process to the supports on the mineshaft walls. The guides are used to guide the vertical movement, while limiting the lateral movements, of the conveyances. This research focuses on the dynamic system where two guides guide the vertical movement (hoisting) of each conveyance. The guides are located on opposite sides of the conveyances. Due to the misalignment of the steel guides, the guides and buntons are susceptible to multiple damaging mechanisms including fatigue damage, plastic deformation of conveyances and derailment from guides. Impact forces on these components could reach 2 to 3 times the gravity load of the conveyance in the form of horizontal impact (Krige 1983). In other words, the magnitude of impact forces can reach 2 to 3 times the weight of the loaded conveyances, which can be in excess of one hundred tons.

During the last few decades, researchers studied multiple mines to calculate the maximum bunton forces and deflections using load cells, strain gauges and computer programs (Krige 1986). The results of these investigations were compiled into a complete guideline to design mineshafts subjected to slam loads (Comro 1990). This guideline was also incorporated into the SANS 10208-4 (2011). In most cases of slam events, the rollers, located on the top and bottom of the conveyance, reduce the impact force exercised by the skip on the steelwork of the mine shaft. Over time, the rollers wear out and become inactive. In turn, the steel slippers mounted on both sides of the skip slam the steel guides directly without dissipating the force causing larger forces on the steelwork. These steel slippers are usually covered with a high-density polyethylene (HDPE) layer to reduce friction between the slipper plate and the guide. Therefore, understanding the dynamic response of skip with inactive rollers is critical. The slam load is primarily influenced by the following:

- Misalignment of the shaft guide.
- The bunton, skip, and guide stiffness.
- The mass of the skip and the hoisting velocity.

To calculate the magnitude of the forces on buntons and deflections of buntons, Comro (1990) transforms the skip and the steel work system into a single degree of freedom (SDOF) system. This SDOF system is formed using an effective mass of the conveyance (m_e) computed about the impact location of the slipper at the leading end of the skip. The system also uses two springs in series representing the skip stiffness (k_s) and the bunton stiffness (k_b). If the skip is very stiff, the total stiffness is considered to be only the bunton stiffness. Finally, the system has an initial velocity equal to impact velocity (u). This SDOF system can be analysed using Newmark's method (Biggs 1964).

To reduce the slamming force, a new slipper design could be developed using a combination of a rubber type material and steel. The rubber material will reduce the effective stiffness of the system which in turn reduces the slamming force on the steel buntons. It will also play an important role for dissipating the dynamic behavior of the steel shaft. The hyper-elasticity of rubber is a useful property for damping dynamic loads. Rubber bearing pads have been used for multiple such applications including mitigating seismic loads and traffic loads on bridges (Roeder and Stanton 1983). Four types of rubber pads are specified in the American Association of State Highway and Transportation Officials (AASHTO 2012): plain unreinforced elastomeric pads (PEP), Fiberglass-Reinforced Pad (FGR), Steel-Reinforced Elastomeric Bearing, and Cotton-Duck-Reinforced Pad (CDP).

This research focuses on CDP which has higher compressive strength than other pad types (Roeder 1999). CDPs consists of thin layers of elastomer and cotton duck fabric. Two main factors should be considered while testing CDP: The pad manufacturer and the shape factor. The shape factor is the ratio between the rubber pad area and its perimeter area. Roeder (1999) tested CDP from three different manufacturers while changing the shape factor and compare the stress- strain curves for the tests. The result showed that shape factors had a negligible effect the stress-strain characteristics compared to changing the manufacturer, as the manufacture specification (MIL-C-882-E 1989) accepts a wide range to tested stresses.

Lehman and Roeder (2005) presented the results of dynamic and fatigue compression tests for CDP samples. Their tests were designed for traffic loads. The test was conducted using 2 million cycles of stress levels equivalent to the heaviest truck loads with a loading rate of 1.5 Hz to avoid heat built up. This test evaluated the durability of the material for 50 to 100 years required for bridge life design. The maximum stress range had the most significant effect on the behavior and failure of the CDPs. To maximize the pad durability, they recommended stress limit of 3 ksi (21 MPa).

Due to the lack of information about the CDP response under impact, this research focused on comparing the static and impact tests to complete a better understanding of the behaviour of CDP under impact. This article presents the CDP tests setup and results. It also includes a guide for designing the flexible slipper based on the CDP test results which will reduce the effective bunton stiffness and the bunton impact force in the mine process.

2 EXPERIMENTAL SETUP

The experimental program consisted of two testing regimes: Static compressive tests and Impact tests. The CDP specimens were cut to 40x40 mm^2 squares with 12.7 mm thickness using a band saw. These 12.7 mm thick pads were bound by epoxy to form three different thicknesses: 12.7, 25.4 and 50.8 mm thick specimens (Figure 1). These three sizes were selected to evaluate the shape factor's effect on the strength of the CDP to be compared to Roeder (1999) results. All specimens were provided by the same manufacturer.

Figure 1: Three specimen sizes: 12.7, 25.4, and 50.8 mm.

2.1 Static compressive test

A universal compression testing machine (UCTM) was used to conduct the low strain rate tests. The testing machine is equipped with a load cell with capacity of 250 kN used to measure the applied loads and two linear variable differential transformers (LVDTs) were used to measure the pad deflection on both sides of the specimen. The specimens were centered between the two LVDTs to maintain an accurate deflection recording. The specimens were, also, centered inside the UCTM to maintain a well distributed load (see Figure 2). Using the computer program associated with the test machine, the loading rate, maximum load, and maximum deflection were specified to maintain a safe and effective test procedures. Before starting a test, the LVDTs and load cell were zeroed to acquire the data starting from zero points. The data from the load cell and the two LVDTs were recorded in tabular form during the test and saved for further analysis. The recorded data was used to construct stress-strain curves for each specimen and loading rate.

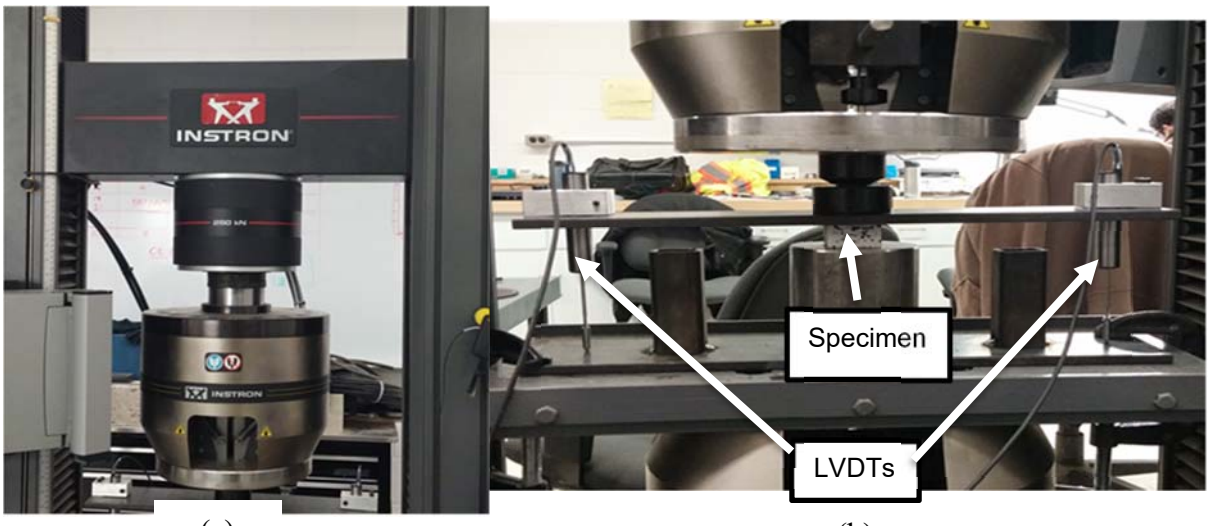

Figure 2: (a) Universal Compression testing machine. (b) LVDTs and experiment set up.

2.2 Impact test

To conduct the impact test, a Charpy impactor was modified by adding a 1” thick steel plate to cover the U-shaped pendulum hammer and adding a non-moving support to hold the specimen to form an impact test machine (Figure 3). A 5000g range accelerometer was mounted on the inner side of the steel plate to measure the applied impact force. A customized full bridge load cell (capacity 320kN) was used to check the data acquired by the accelerometer at the non-moving support (Figure 3).

The Charpy machine provides two release positions for the pendulum hammer. The two release positions were used to provide different impact forces to measure the rubber properties under higher strain rates (Figure 4).

For this test, the specimen was speckled by coloring the surface with white color and using a black spray to form a random pattern of black and grey dots. A high-speed camera was used to capture images of the specimen during the test at a rate of 5000 frame/s. Using the images captured by the camera a digital image correlation (DIC) was used to acquire the deflection of the specimen. The test was conducted as follows:

- The specimen was mounted to the non-moving support plate perpendicular to the hammer.
- The high-speed camera was adjusted to the same height as the specimen to acquire images perpendicular to the specimen surface for analysis.
- The accelerometer and the load cell were connected to a data acquisition system.
- The hammer was latched to either of the two positions.
- The hammer was released and the data from the camera and sensors is recorded.

The final acquired data was used to build a stress-strain curve for the loading and unloading for each specimen.

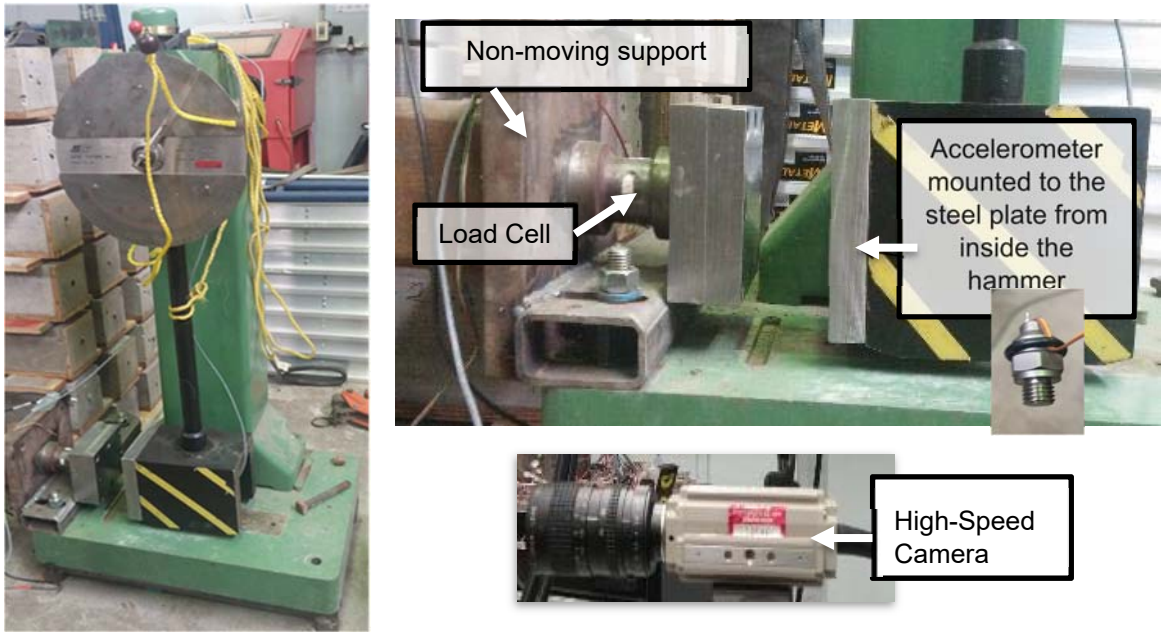

Figure 3: Overall set up for accelerometer, load cell, and high-speed camera in modified Charpy testing machine.

Figure 4: Two pendulum hammer positions for the Charpy machine.

3 TEST RESULTS AND DISCUSSION

3.1 Static compressive test

To understand the behavior of the CDP material under static compression test, seven tests were conducted using the procedure presented earlier. Each test had a different thickness and/or loading rate. In the first four tests, 12.7 mm thick specimens were used while increasing the loading rate. In test 5 and 6, 25.4 mm thick specimens with two different loading rates. Finally, for test seven, 50.8 mm specimens were used. Figure 5 presents the average stress-strain curves for each of the seven tests. The test was displacement controlled. The speed of the machine varied from one test to another. Accurate strain rates for each test were calculated based on the average displacement readings from the two LVDTS, the measured thickness of the samples, and the time of the test. The calculated strain rates were used to compare the behavior of the material.

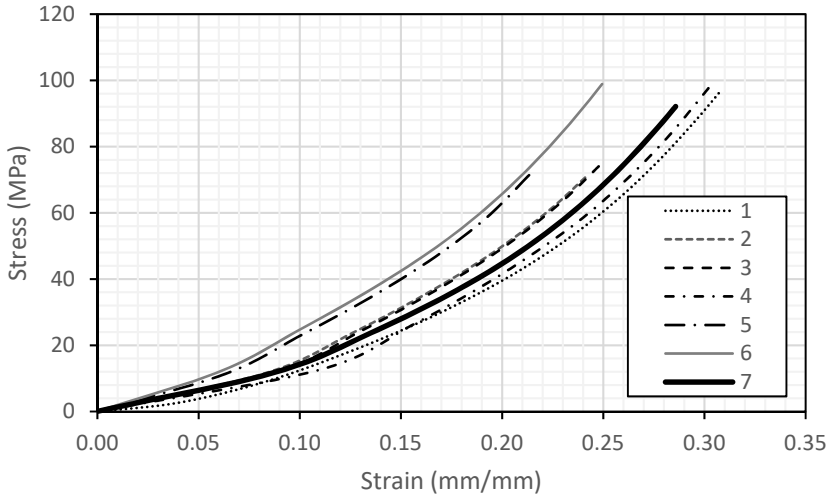

Figure 5: Average Stress-strain curves compared for the 7 static compressive tests.

The stress-strain curves, presented in Figure 5, shows the non-linear behavior of the CDP. The modulus of elasticity is increasing while increasing the stress. Figure 6 presents the relation between the tangent modulus of elasticity and the strain rates at stresses 20, 45, and 70 MPa. These stresses present the limits as provided by AASHTO standards (2012). The maximum allowable stress for CDP required by AASHTO is 20MPa (3ksi), the minimum failure stress for CDP as required by AASHTO (2012) is 70 MPa (10ksi), and 45 MPa was used to improve the analysis of the CDP behavior. Tangent modulus (E_T) at stress equal 20 MPa was found approximately equal 300 MPa. Comparing the values of E_T at 45 MPa, the modulus of elasticity of the seven tests was found approximately equal 400 MPa. Followed by E_T at 70 MPa was approximately equal to 600 MPa. In general, the small changes in strain rates did not affect major changes to the material properties. Additional CDP thicknesses should be tested to investigate the behavior and compare more CDP shape factors and strain rates.

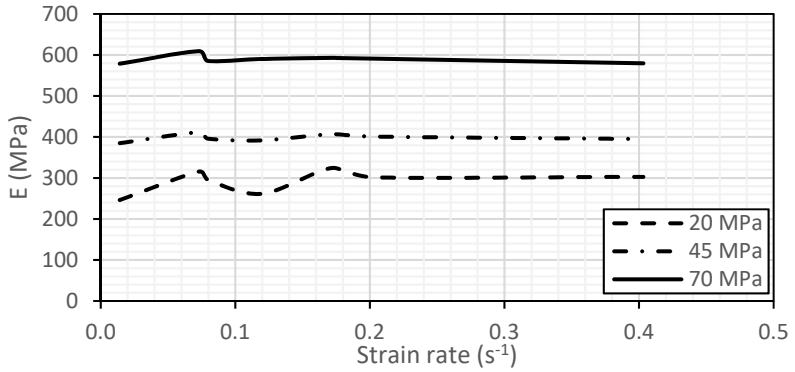

Figure 6: The modulus of elasticity E_T values for the static test for each strain rate calculated at stresses 20, 45, & 70 MPa.

3.2 Impact test

To understand the behavior of the CDP material under impact test, a comparison between the 6 conducted tests is presented in this section. Each test had a different thickness and/or Charpy position. Test 8 & 9 used 12.7 mm thick specimen, 25.4 mm thick were used for tests 10 &11, and 50.8 mm for test 12 & 13. Figure 7 presents the average stress-strain curves for all tests compiled. In this test, the strain rates were calculated as the ratio between the maximum specimen strain and the total time between the hammer hitting the specimen and the specimen reaching the maximum deflection. The strain rate for each test, the displacement acquired from DIC analysis, the measured thickness of the samples, and the accelerometer data, were used to compare the stress-strain results and the modulus of elasticity (E_T). The ascending branch of the stress-strain data could be presented by a second-degree polynomial regression curve. The secant modulus of elasticity (E_S) was calculated as the derivative of the second-degree curve as presented in Table 1.

The calculated E values, presented in Figure 8, shows the non-linear behavior of the CDP and the relation between E and the strain rates at stresses 20, 45, 70 & 100 MPa. Elastic modulus (E_T) at stress equal 20 MPa was found between a value of 340 to 420 MPa. This wide range for the modulus of elasticity values proves that the strain-rate play an important role in changing the CDP behavior. Elastic modulus (E_T) was generally increasing while the strain rate increased from 41.995 to 119.190 s^{-1} followed by a reduction at strain-rate equal to 193.74 s^{-1}. Comparing the values of E_T at 45 MPa, the modulus of elasticity of the six tests was found to be between 480 to 620 following the same increase and decrease behavior as the behavior presented in the modulus of elasticity calculated at 20 MPa. Modulus of elasticity (E_T) at 70 MPa was ranged between 700 and 770 MPa following the same behavior. Finally, (E_T) at 100 MPa was between 830 and 860 for tests 9 and 11. In general, the change in strain rates affected the behavior of CDP in this impact test. Additional CDP thicknesses should be tested to investigate the behavior and compare more CDP shape factors and strain rates.

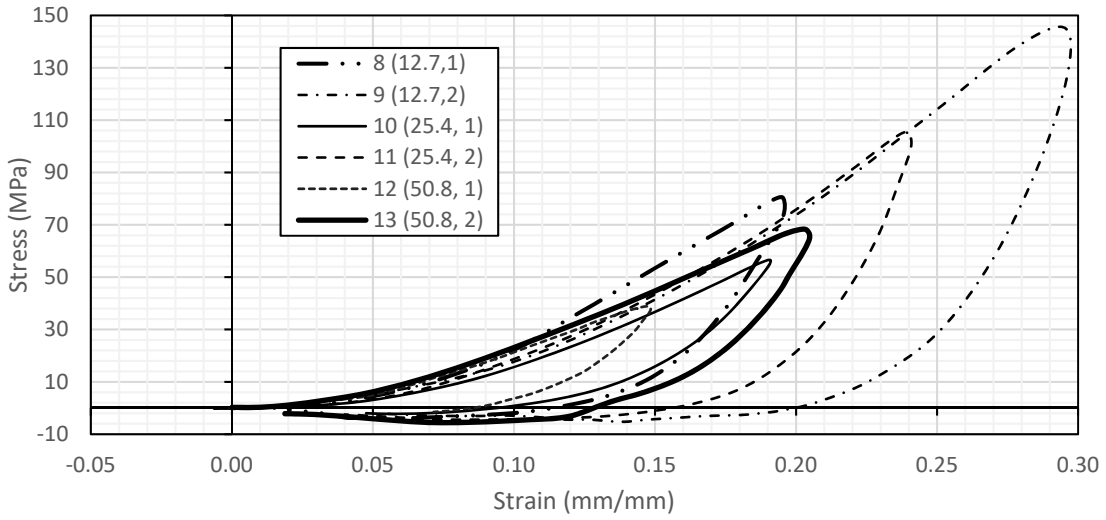

Figure 7: Stress-strain curves compiled for the 8 sets of impact tests.

Table 1: Stress second-degree polynomial, secant modulus of elasticity equation (E) and R^2, where ε is the strain.

Test number	Stress function (σ) (MPa)	Secant modulus of elasticity equation (E) (MPa)	R^2
8	$2144.5\varepsilon^2 + 16.565\varepsilon$	$2144.5\varepsilon + 16.565$	0.9969
9	$1869.7\varepsilon^2 - 5.3779\varepsilon$	$1869.7\varepsilon - 5.3779$	0.9999
10	$1674.9\varepsilon^2 - 10.47\varepsilon$	$1674.9\varepsilon - 10.47$	0.9994
11	$1967\varepsilon^2 - 11.557\varepsilon$	$1967\varepsilon - 11.557$	0.9995
12	$1845.8\varepsilon^2 + 23.151\varepsilon$	$1845.8\varepsilon + 23.151$	0.9985
13	$1306.4\varepsilon^2 + 95.018\varepsilon$	$1306.4\varepsilon + 95.018$	0.9976
Average	$1984.5\varepsilon^2 - 15.446\varepsilon$	$1984.5\varepsilon - 15.446$	0.9745

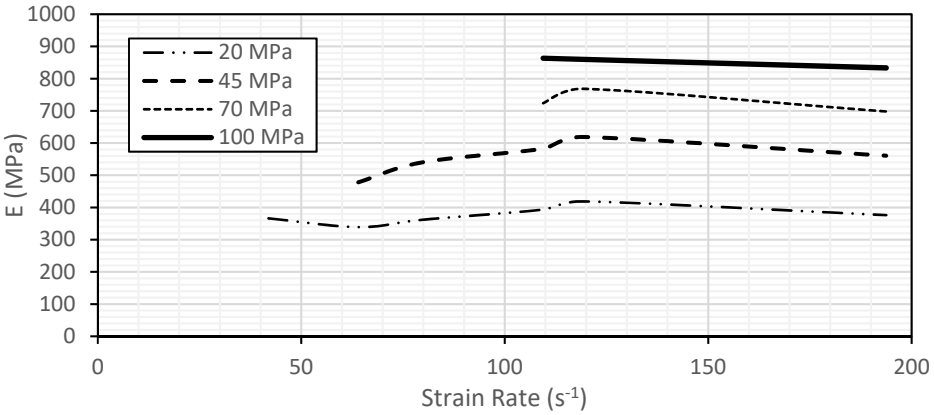

Figure 8: The modulus of elasticity (E_T) values for the impact test for each strain rate calculated at stresses (20, 45, 70, & 100).

In general, the modulus of elasticity increases with increasing the strain rate. At stress equal to 20 MPa, the modulus of elasticity increased from a value of 300 MPa at strain rates 0 to 0.4 s^{-1} to values from 340 to 420 MPa at strain rates between 40 & 200 s^{-1}. This increase is 15% to 40% increase in E depending on the strain rate. At a stress equal to 45 MPa, E increased from a value of 400 MPa at strain rates 0 to 0.4 s^{-1} to values from 480 to 620 MPa at strain rates between 40 & 200 s^{-1}. This increase represents a 20% to 55% increase in E depending on the strain rate. At a stress equal to 70 MPa, E increased from a value of 600 MPa at strain rates 0 to 0.4 s^{-1} to values from 700 to 780 MPa at strain rates between 40 & 200 s^{-1}. This increase is a 17% to 30% increase in E depending on the strain rate. The maximum percentage increase in E is calculated equal to 50%.

3.3 The new slipper design using the SDOF Newmark's method

The new slipper design is based on creating a lower effective bunton stiffness by adding an elastomer pad with low stiffness to the effective bunton stiffness in series (see Figure 9). The final effective stiffness can be calculated by adding the pad stiffness to the original effective stiffness in series as presented in Equation 1.

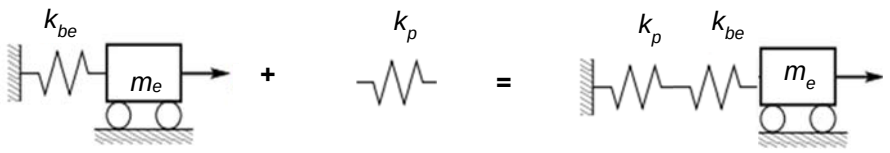

Figure 9: The addition of the elastomer pad stiffness to a SDOF system to form a new SDOF system.

[1] $k_{pbe} = \frac{k_{be}k_p}{k_{be}+k_p}$

Where: k_{be} is the effective bunton stiffness, k_p is the elastomer pad stiffness, and k_{pbe} is the combined effective stiffness.

Using the CDP test results, a SDOF program was used to obtain a new dynamic response including the calculation of the maximum bunton force. Two methods were used in calculating the pad stiffness:

- The CDP stiffness function obtained by multiplying the pad modulus of elasticity's function (E_p) by the ratio between the pad area (A) and thickness (t) (Equation 2).
  [2] $k_p = \frac{E_p A}{t}$
  Where: *A* is the pad area and *t* is the pad thickness.
- To facilitate the design procedures, constant value for E_p (E^*) can be calculated using conservation of energy method, where the area under the pad stress-strain curve is equal to the area under the curve created by a constant value E^* at a given stress value. For maximum stress of 20 MPa, E^* equal to 300 MPa could be used.

Table 2 presents the modulus of elasticity equations created for each dynamic test performed in the previous section. Using Equation 2, k_p functions were calculated by the E_p functions presented in the table.

The k_p functions were used in the numerical integration (Newmark's method) to evaluate the effect of adding k_p in series to the bunton effective stiffness. Multiple trials were performed while changing the area and thickness of the CDP used to reduce the bunton force and guide displacement.

Table 2: E_p modulus of elasticity and pad stiffness k_p based on secant calculations (where: *u* is the pad deflection, *A* is the pad area, and *t* is the pad thickness).

Test number	Modulus of elasticity equation (E_p) (MPa)	Pad Stiffness k_p (N/m)
8	2144.5ε + 16.57	$(2.145\text{x}10^9 \frac{u}{t} + 16.57\ \text{x}10^6) \frac{A}{t}$
9	1869.7ε - 5.38	$(1.870\ \text{x}10^9 \frac{u}{t} - 5.38\ \text{x}10^6) \frac{A}{t}$
10	1674.9ε - 10.47	$(1.675\text{x}10^9 \frac{u}{t} - 10.47\ \text{x}10^6) \frac{A}{t}$
11	1967.0ε - 11.56	$(1.967\text{x}10^9 \frac{u}{t} - 11.56\ \text{x}10^6) \frac{A}{t}$
12	1845.8ε + 23.15	$(1.846\text{x}10^9 \frac{u}{t} + 23.15\ \text{x}10^6) \frac{A}{t}$
13	1306.4ε + 95.02	$(1.306\text{x}10^9 \frac{u}{t} + 95.02\ \text{x}10^6) \frac{A}{t}$
Average	1984.5ε - 15.45	$(1984.5\text{x}10^9 \frac{u}{t} - 15.45\ \text{x}10^6) \frac{A}{t}$

Comparing the results of adding the CDP to the system, the following was found:

- Reducing the area and increasing the thickness of the pad decreases the total pad stiffness which reduces the bunton force.
- The pad stiffness had to be reduced considerably to show a significant effect on the bunton force. Using lage areas and smaller pad thickness was not effective. On the other hand, using CDP washers with smaller area and larger thickness reduced the impact force.

4 DESIGN APPROACH

Using the results of the tests performed on CDP, the new slipper design was created using CDP between the slipper's steel plate and the skip body. This new system reduced the effective bunton stiffness which reduced the maximum bunton force. To facilitate the new design procedures, a constant modulus of elasticity (E^*) was introduced to create a linear system instead of a non-linear system represented by a second-degree polynomial equation. The designer starts by finding the maximum bunton force from the analysis of the original system using SANS 10208-4 (2011). Using the calculated maximum force and maximum allowable stress, allows the designer to select the area of the pad needed to keep the pad stress level below the allowable stress limit. Then, a pad thickness is selected depending on the allowed distance between the slipper plate and the guide surface. The pad stiffness (k_p) is calculated using the pad area and thickness previously obtained and E^* value. A new effective bunton stiffness is then calculated and a new bunton force is obtained using SANS 10208-4 (2011). The results of this method were compared to the results of using numerical integration of time history for a single degree of freedom system while using the non-linear pad behavior.

5 CONCLUSION

This research was conducted to improve the skip side slippers design. The new slipper design provides information about how to reduce slam loads in mineshafts of deep mines. Slam loads are highest when there is steel-to-steel contact between the slippers and the shaft rails. This hard contact has the most harmful effect on the steelwork of the mineshaft.

To increase the productivity of a mine, the mass and the velocity of the skip should be maximized. A high mass and high velocity system could result in high slam loads, requiring stronger steelwork for the mineshaft. This would likely also result in a stiffer mineshaft rail system, which has the effect of further increasing potential slam loads. An alternative to increasing capacity of the rails is to reduce the effective stiffness of the skip/guide system. This reduction in stiffness will reduce the maximum bunton force. One way to reduce stiffness is to provide an additional flexible material at the slipper location that acts in series with the skip and rail system. This flexible slipper reduces the effective bunton stiffness and therefore the bunton impact force.

Cotton Duck Pads (CDP), used as bearing pads in multiple applications, were tested to examine their behavior under static and dynamic compression loads. The tests reported the results for both types of tests for CDP and described the material with a focus on the change of modulus of elasticity with changing the strain rate. The results from both tests are described by the following:

- As expected, the modulus of elasticity increases with increasing the strain rate.
- The modulus of elasticity can be represented by a second-degree polynomial curve, which could be simplified by secant value of E.

Acknowledgements

This was conducted with the financial and in-kind support of NSERC and Stantec Consulting Ltd., for which the authors express their gratitude.

References

American Association of State Highway and Transportation Officials, 2012. AASHTO LRFD bridge design specifications. Washington, D.C, USA.

Biggs, J.M., 1964. *Structural Dynamics*. McGraw-Hill, New York, NY, USA.

Chamber of Mines Research Organization (COMRO) 1990. User Guide No. 21: *Design guidelines for the dynamic performance of shaft steelwork and conveyances*. Auckland Park: COMRO.

Cloth, Duck, cotton or cotton-polyester blend, synthetic rubber, impregnated and laminated, oil resistant 1989 *MIL-C-882E*

Krige G. J. , 1983, Thesis: *The Behaviour and Design of Mineshaft steelwork and conveyances*. University of the Witwatersrand, Johannesburg, South Africa.

Krige G. J., 1986, Some initial findings on the behaviour and design of mine-shaft steelwork and conveyances. *Journal of the south African institute of mining and metallurgy*, **86** (6): 205-215.

Lehman, D. E., Roeder, C.W., Larsen, R.A., 2005 Design of cotton duck bridge bearing pads *Journal of Bridge Engineering*, **10** (5): 555-563.

Roeder, C. W., and J. F. Stanton. 1983. Elastomeric Bearings: A State of the Art. *Journal of the Structural Division: American Society of Civil Engineers* **109** (12): 2853–2871.

Roeder, C. W. 1999. *LRFD design criteria for cotton duck pad _CDP_ bridge bearing. Final Rep. on NCHRP Project 20-07/99, National Cooperative Highway Research Program*, Transportation Research Board, National Research Council, Washington, D.C, USA.